View metadata, citation and similar papers at core.ac.uk
brought to you by CORE
provided by DSpace@MIT

Conformal Field Theory of Critical Casimir Interactions in 2D

Giuseppe Bimonte,[1,2] Thorsten Emig,[3] and Mehran Kardar[4]
[1] *Dipartimento di Scienze Fisiche, Università di Napoli Federico II, Complesso Universitario MSA, Via Cintia, I-80126 Napoli, Italy*
[2] *INFN Sezione di Napoli, I-80126 Napoli, Italy*
[3] *Laboratoire de Physique Théorique et Modèles Statistiques, CNRS UMR 8626, Bât. 100, Université Paris-Sud, 91405 Orsay cedex, France*
[4] *Massachusetts Institute of Technology, Department of Physics, Cambridge, Massachusetts 02139, USA*
(Dated: July 16, 2013)

Thermal fluctuations of a critical system induce long-ranged Casimir forces between objects that couple to the underlying field. For two dimensional (2D) conformal field theories (CFT) we derive an exact result for the Casimir interaction between two objects of arbitrary shape, in terms of (1) the free energy of a circular ring whose radii are determined by the mutual capacitance of two conductors with the objects' shape; and (2) a purely geometric energy that is proportional to conformal charge of the CFT, but otherwise super-universal in that it depends only on the shapes and is independent of boundary conditions and other details.

PACS numbers: 12.20.-m, 03.70.+k, 42.25.Fx

arXiv:1307.3993v1 [cond-mat.stat-mech] 15 Jul 2013

Objects embedded in a medium constrain its natural fluctuations, resulting in fluctuation-induced forces [1]. The most naturally occurring examples result from modification of electromagnetic fluctuations, manifested variously in van der Waals interactions [2] (between atoms and molecules) to Casimir forces (between conducting plates) [3]. While fluctuations of the latter are primarily quantum in origin, thermal fluctuations of correlated fluids lead to similar interactions, most notably at a critical point (where correlation lengths are macroscopic) [4, 5]. Critical fluctuation-induced forces have been observed in helium [6] and in binary liquid mixtures [7–9] Critical fluctuations of a binary mixture were recently employed to manipulate and assemble colloidal particles [10].

Biological membranes are mainly composed of mixtures of lipid molecules, and could potentially be poised close to a critical point demixing point [11, 12], in the two-dimensional Ising universality class. It has been suggested that membrane concentration fluctuations could thus lead to critical Casimir forces between inclusions on such membranes, motivating computation of such forces between discs embedded in the critical Ising model [13]. Membranes (and interfaces) also undergo thermal shape fluctuations governed by the energy costs of bending (and surface tension) [14]. Modification of these fluctuations have also been proposed as a source of interactions amongst inclusions on membranes [15, 16], possibly accounting for patterns of colloidal particles at an interface [17]. There is extensive literature on this topic, and the interested reader can consult recent publications [18, 19]. Yet another entropic force is proposed to act between surface/membrane bio-adhesion bonds [20].

Conformal field theories (CFTs) have proved highly successful in studies of two dimensional (2D) systems at criticality [21, 22]. Various boundary conditions have been examined for Ising (or 3-state Potts) model on a cylinder [23]. Connections to Casimir forces between parallel plates [24, 25] and spheres [26, 27] have been explored. Non-spherical particles at large separations have been studied with the small particle operator expansion [28, 29]. However, a general formulation for interactions between two (or more) objects of arbitrary shape embedded in a CFT appears to be lacking. Some special cases recently studied include interactions between two spherical holes in a free field [30], between circular inclusions [13] and needles [31] in a critical Ising system. (We note in passing exact solutions for Casimir interactions between spheres in three dimensions [26, 27, 32].) Starting with the solution of the Laplace equation with two inclusions of arbitrary shape as equipotentials, the system can be conformally mapped either to a cylinder, or an annulus. We demonstrate that such mapping can be employed to compute the Casimir interaction between the two objects embedded in any CFT.

We consider a general two dimensional classical field theory with an energy that is invariant under conformal transformations. Examples include free theories, such as the capillary-wave Hamiltonian that describes deformations with small gradients around a flat interface, and interacting theories, like the Ising model at its critical point. The corresponding CFT is assumed to couple to two compact objects covering areas S_1 and S_2 via conformally invariant boundary conditions on the boundaries ∂S_α ($\alpha = 1$ or 2). Examples include Dirichlet or Neumann conditions for a free field, and pinned or free conditions for the Ising model. In the following we assume that the boundaries ∂S_α are Jordan curves [40].

Before explaining the main steps of the derivation, and presenting examples, we summarize our main result: The doubly connected domain bounded by ∂S_1 and ∂S_2 can be conformally mapped to the surface of a cylinder with unit radius and length ℓ, or alternatively to an annulus with outer and inner radii of 1 and $e^{-\ell}$, respectively, see Fig. 1. The map $w(z)$ to the cylinder has an electrostatic interpretation: The real (and imaginary) part of the map is $2\pi/Q$ times the electrostatic potential (and its conjugate function) outside the objects with the potential set to -1 for ∂S_1, and 0 for ∂S_2, with net charges of $-Q$ and $+Q$, respectively [33]. The cylinder length $\ell = 2\pi/C$ is then given by the mutual capacitance C of two cylindrical conducting surfaces in 3D that have the areas S_j as their cross section. The map to the annulus is then $\tilde{w}(z) = \exp[w(z)]$. Our main result is that the x and y components of the Casimir force between the two objects are combined into the complex force

$$F \equiv \frac{F_x - iF_y}{2} = -\partial_\zeta \mathcal{F}_{\text{ann.}} - \frac{ic}{24\pi}\oint_{\partial S_2}\{\tilde{w}, z\}dz\,. \qquad (1)$$

In the first contribution above, $\mathcal{F}_{\text{ann.}}$ is the free energy of the CFT on the annulus with the boundary conditions of ∂S_1 (∂S_2) on the inner (outer) circle (see below for examples); and the derivative is with respect to $\zeta = (x_2 - x_1) + i(y_2 - y_1)$, the distance in the complex plane between two origins (x_α, y_α) on the objects. (Note that throughout the paper we set $k_B T = 1$, such that $\mathcal{F} = -\ln Z$.) The second term is proportional to c, the conformal charge of the CFT, and involves the integral of the Schwarzian derivative [34] of the conformal map $\tilde{w}$, $\{\tilde{w}, z\} \equiv (\tilde{w}'''/\tilde{w}') - (3/2)(\tilde{w}''/\tilde{w}')^2$, along the counter ∂S_2 performed counter-clockwise. This contribution to the force can be written in terms of a 'geometric' free energy as $F_{\text{geo}} = -c\partial_\zeta \mathcal{F}_{\text{geo.}}$. $\mathcal{F}_{\text{ann.}}$ varies with the CFT but depends on geometry only through the capacitance via $\ell = 2\pi/C$. By contrast $\mathcal{F}_{\text{geo.}}$ is fully determined by the shape of the objects, independently of the CFT. In this sense, F_{geo} is *super-universal* as it is the same for all CFT's (up to a factor of c). It vanishes if and only if $\tilde{w}$ is a *global* conformal map, i.e., when the objects S_α are circular. This follows as the Schwarzian derivative measures the deviation of the map from being global.

Sketch of proof — We begin by relating the change in the cylinder length ℓ with the objects separation ζ, to the map $w(z)$. After a small displacement of S_2, the electrostatic energy is modified by

$$\delta\mathcal{E}_{\text{el}} = \frac{1}{2\pi i}\oint_{\partial S_2} \alpha(z)\, T_{\text{el}}(z) dz + \text{c.c.}\,, \qquad (2)$$

where $\alpha(z)$ reverses the motion. The electrostatic stress tensor is well known and can be expressed in terms of the cylinder map $w(z)$ by $T_{\text{el}}(z) = -(\pi/2)(\partial_z w)^2$. Since at fixed charges $Q = \pm 2\pi$, $\delta\mathcal{E}_{\text{el}} = -(2\pi)^2\delta(1/2C)$, and $\ell = 2\pi/C$, $\delta\ell = -\delta\mathcal{E}_{\text{el}}/\pi$. By applying Eq. (2) within S_2 with $\alpha = -\delta x$ and $\alpha = -i\delta y$, and setting $\partial_\zeta \ell = (\partial_x \ell - i\partial_y \ell)/2$, we then find $\partial_\zeta \ell = (i/4\pi)\oint_{\partial S_2}(\partial_z w)^2 dz$.

The displacement of S_2 changes the Casimir free energy by an amount $\delta\mathcal{F}$, also given by Eq. (2) with T_{el} replaced by the stress tensor $T(z)$ of the CFT outside

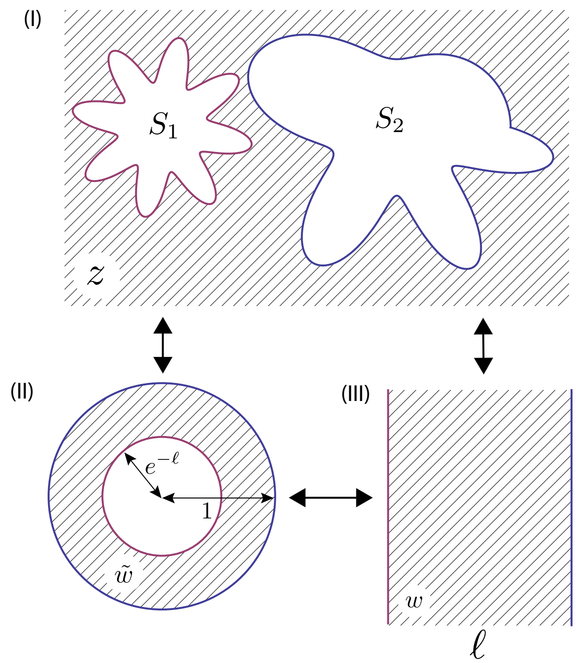

FIG. 1: Conformal maps of the exterior region of two objects S_1 and S_2 to an annulus via $\tilde{w}(z)$, and to the surface of a cylinder by $w(z)$ (see text for details).

the objects. To obtain a simple expression for $T(z)$ in terms of the above maps we proceed as follows: As in Eq. (2), the stress tensor for the cylinder can be expressed in terms of the derivative of the free energy with respect to its length by $2T(w) = \partial_\ell \mathcal{F}_{\text{cyl.}} = \partial_\ell \mathcal{F}_{\text{ann.}} - c/12$. For the second form, we have relied on a known relation $\mathcal{F}_{\text{cyl.}} = \mathcal{F}_{\text{ann.}} - \ell c/12$ between the cylinder and annulus free energies [22, 34]. Next, we note that for any map $w(z)$, the stress tensor transforms according to $T(z) = (\partial_z w)^2 T(w) + (c/12)\{w, z\}$ [34]. We can use this expression to relate $T(\tilde{w})$ to $T(w)$, and separately to relate $T(z)$ to $T(\tilde{w})$, to finally obtain $T(z) = (1/2)(\partial_z w)^2 \partial_\ell \mathcal{F}_{\text{ann.}} + (c/12)\{\tilde{w}, z\}$. Using this result in Eq. (2) both with $\alpha = -\delta x$ and $\alpha = -i\delta y$ we arrive at Eq. (1) after using the previous expression for $\partial_\zeta \ell$.

Asymptotic limits of the annulus free energy — The scaling of $\mathcal{F}_{\text{ann.}}$ for small and large $\ell = 2\pi/C$ (and hence short and large separations $|\zeta|$) can be obtained from two equivalent representations of one-dimensional quantum field theories (QFT's) (page 423 of Ref. [34]). First, consider the QFT on a circle of circumference δ with Hamiltonian $\hat{H} = (2\pi/\delta)(\hat{L}_0 + \hat{\bar{L}}_0 - c/12)$ where $\hat{L}_0$, $\hat{\bar{L}}_0$ are Virasoro generators in the plane. The euclidean space-time of the QFT forms a cylinder with length ℓ in the time direction, whose classical free energy is $\mathcal{F}_{\text{cyl}} = -c(\pi/6)(\ell/\delta) + \mathcal{F}_{\text{ann.}}$, with $\mathcal{F}_{\text{ann.}} = -\ln\langle a|\exp(-2\pi(\ell/\delta)(\hat{L}_0 + \hat{\bar{L}}_0))|b\rangle$ and boundary states $|a\rangle$, $|b\rangle$. The first term $\sim \ell$ is the extensive part of the cylinder energy, given by the ground state of the QFT.

If the lowest eigenvalue of $\hat{L}_0 + \hat{\bar{L}}_0$ is zero (e.g. in unitary CFT's), for $\ell \gg \delta \equiv 2\pi$ one has $\mathcal{F}_{\text{ann.}} \sim e^{-\eta\ell/2}$ where $\eta/2$ is the smallest positive eigenvalue of $\hat{L}_0 + \hat{\bar{L}}_0$ that couples to $|a\rangle$ and $|b\rangle$ [41]. The decay of the two-point correlation function of the corresponding scaling field in unbounded space is also governed by the exponent η. Since $\ell \to 2\ln|\zeta|$ for large distance, we arrive at $\mathcal{F}_{\text{ann.}} \sim |\zeta|^{-\eta}$ [28, 29].

Next, consider the QFT on an interval of length ℓ with the Hamiltonian $\hat{H} = (\pi/\ell)(\hat{L}_0 - c/24)$. The cylinder is obtained as the euclidean space-time of the QFT by choosing the time direction now along the circumference δ. For $\ell \ll \delta = 2\pi$ this yields $\mathcal{F}_{\text{cyl}} = -c(\pi/24)(\delta/\ell) - \ln \text{Tr} e^{-\pi(\delta/\ell)\hat{L}_0}$. If the smallest eigenvalue of $\hat{L}_0$ is $\tilde{\eta}/2$, for $\ell \to 0$ one has $\mathcal{F}_{\text{ann.}} \to \pi^2(\tilde{\eta} - c/12)/\ell$. Since ℓ is given by the mutual capacitance, one has for smooth surfaces the short distance expansion

$$\frac{1}{\ell} = \sqrt{\frac{R_1 R_2}{2(R_1+R_2)d}} + \frac{R_1^3 + R_2^3}{12(R_1+R_2)^{5/2}}\sqrt{\frac{d}{2R_1R_2}} + \mathcal{O}(d^{3/2}), \tag{3}$$

where R_α are the local radii of curvature at the closest points of the boundaries ∂S_α with separation d.

Asymptotic limits of the geometric free energy — The geometric contribution $\mathcal{F}_{\text{geo.}}$ is independent of the CFT, and solely related to the electrostatic potential through the map $\tilde{w}(z) = e^{w(z)}$. The large distance behavior of F_{geo} can be obtained from a multipole expansion with respect to origins Z_α inside S_α, which yields the convergent bipolar series [35]

$$w(z) = \ln\frac{z - Z_1}{z - Z_2} + \sum_{m=1}^{\infty} \frac{1}{m}\left[\frac{\hat{Q}_{1,m}}{(z-Z_1)^m} - \frac{\hat{Q}_{2,m}}{(z-Z_2)^m}\right], \tag{4}$$

where coefficients $\hat{Q}_{\alpha,m}$ can be expressed in terms of the electrostatic T-matrix elements of the objects and so-called translation matrix elements that couple multipole moments (MM) on different objects [36]. This yields a distance $\zeta = Z_2 - Z_1$ dependence of the form $\hat{Q}_{\alpha,m} = q_{\alpha,m,1} + q_{\alpha,m,2}/\zeta + \mathcal{O}(\zeta^{-2})$. We expand the Schwarzian derivative $\{\tilde{w}, z\}$ for large $z - Z_\alpha$ and move the contour integration of Eq. (1) to the y-axis. With $\text{Re}(Z_1) < 0$, $\text{Re}(Z_2) > 0$, this yields to leading order at large distance

$$F_{\text{geo}} = -\frac{(\hat{Q}_{1,1}^2 + \hat{Q}_{1,2})(\hat{Q}_{2,1}^2 + \hat{Q}_{2,2})}{\zeta^5} + \mathcal{O}(\zeta^{-6}). \tag{5}$$

In most cases of interest the ζ^{-5} decay of F_{geo} is subdominant to $\zeta^{-(\eta+1)}$ coming from $F_{\text{ann.}}$. There can, however, be exceptions [21] with $\eta > 4$ where the geometric force is dominant.

The short distance behavior of F_{geo} is more complex. On physical grounds we expect that the net Casimir force is dominated by points of closets approach. In the so called proximity force approximation (PFA) [2, 37], the force between *smoothly varying surfaces* is obtained by integrating the pressure for parallel plates, evaluated at local separations. This procedure is indeed consistent with the short-distance contribution from $F_{\text{ann.}} \equiv -\partial_\zeta \mathcal{F}_{\text{ann.}}$ that follows from Eq. (3). However, there is no corresponding 'parallel plate pressure' for the geometric force, since the $\tilde{w}(z)$ is now a global conformal map with $\{\tilde{w}, z\} = 0$. (For the same reason $F_{\text{geo}} = 0$ between two circles.) For PFA to remain valid, any contribution of F_{geo} should be sub-leading to $F_{\text{ann.}}$ as $d \to 0$, and we believe that F_{geo} approaches a shape-dependent constant in this limit. PFA is not expected to hold for non-smooth surfaces, such as those with sharp corners or tips. Indeed, for the case of needles (discussed below), we find that both F_{geo} and $F_{\text{ann.}}$ scale as $1/d$ for $d \to 0$.

Free energy of the annulus for specific models — The free energy for an annulus is known exactly for certain CFTs. For the free Gaussian field of a surface tension dominated interface (with infinite capillary length), the free energy $\mathcal{F}_{\text{ann.}}$ on the annulus can be expressed in terms of the Dedekind eta function $\eta(\tau) = e^{i\pi\tau/12}\prod_{n=1}^{\infty}(1 - e^{2\pi i n\tau})$ which is defined on the upper complex τ-plane. One then obtains

$$\mathcal{F}_{\text{ann.,D}} = \frac{\pi}{6C} + \frac{1}{2}\ln\left(\frac{2\pi}{C}\right) + \ln\eta\left(\frac{2i}{C}\right), \tag{6}$$

$$\mathcal{F}_{\text{ann.,N}} = \frac{\pi}{6C} + \ln\eta\left(\frac{2i}{C}\right), \tag{7}$$

for Dirichlet and Neumann conditions, respectively, and dropping an unimportant constant for the former. For small C (large separations), this leads to $\mathcal{F}_{\text{ann.,D}} \approx \mathcal{F}_{\text{ann.,D,small C}} = (1/2)\ln(2\pi/C)$ and $\mathcal{F}_{\text{ann.,N}} \approx \mathcal{F}_{\text{ann.,N,small C}} = -e^{-4\pi/C}$. This distinct behavior at large separations follows from the absence of monopoles for Neumann boundary conditions. The Neumann result corresponds to $\eta = 4$ and thus $\mathcal{F}_{\text{ann.}}$ scales the same way at large separations as $\mathcal{F}_{\text{geo}}$. For large C (small separations) an expansion to *all orders* yields the simple forms

$$\mathcal{F}_{\text{ann.,D,large C}} = \frac{\ln\pi}{2} - \frac{\pi}{24}C + \frac{\pi}{6}\frac{1}{C}, \tag{8}$$

$$\mathcal{F}_{\text{ann.,N,large C}} = \frac{1}{2}\ln\frac{C}{2} - \frac{\pi}{24}C + \frac{\pi}{6}\frac{1}{C}. \tag{9}$$

The accuracy of the approximations for small and large C is remarkable, with maximum errors of roughly 0.32% and 1.6% for Dirichlet and Neumann cases respectively.

For $c = 1/2$, CFT describes the continuum limit of the critical Ising model. The free energy of the annulus depends on the boundary conditions. For fixed spins on the boundaries, one has

$$\mathcal{F}_{\text{ann.},\pm} = \frac{\pi}{12C} - \ln\left[\chi_0\left(\frac{2i}{C}\right) + \chi_{\frac{1}{2}}\left(\frac{2i}{C}\right) \pm \sqrt{2}\chi_{\frac{1}{16}}\left(\frac{2i}{C}\right)\right],$$

with upper (lower) sign for like (unlike) boundary conditions and with Virasoro characters

$\chi_0(\tau) = [\sqrt{\theta_3(\tau)/\eta(\tau)} + \sqrt{\theta_4(\tau)/\eta(\tau)}]/2$, $\chi_{\frac{1}{2}}(\tau) = [\sqrt{\theta_3(\tau)/\eta(\tau)} - \sqrt{\theta_4(\tau)/\eta(\tau)}]/2$, $\chi_{\frac{1}{16}}(\tau) = \sqrt{\theta_2(\tau)/(2\eta(\tau))}$, where $\theta_j(\tau) \equiv \theta_j(0|\tau)$ are Jacobi theta functions [34]. At large distance ℓ one has $\mathcal{F}_{\text{ann.},\pm} \to \mp\sqrt{2}e^{-\ell/8}$, and for vanishing ℓ the limits $\mathcal{F}_{\text{ann.},+} \to -\pi^2/(24\ell)$ and $\mathcal{F}_{\text{ann.},-} \to 23\pi^2/(24\ell)$. Both are consistent with the predicted asymptotic behaviors with $\eta = 1/4$, $\tilde{\eta}_+ = 0$, and $\tilde{\eta}_- = 1$.

Examples — We illustrate the power of our general result with two examples for the free Gaussian field of the interface (capillary wave) Hamiltonian for which $c = 1$. The first case consists of two circles of equal radii R and center-to-center separation D, as in Fig. 2(a). This is the only (compact) geometry for which the geometric force F_{geo} vanishes. The mutual capacitance is $C = 2\pi/\text{arccosh}[\frac{1}{2}(D/R)^2 - 1]$, [38] and substitution into Eq. (6) yields at small surface-to-surface separation $d = D - 2R \ll R$, the Dirichlet Casimir free energy

$$\mathcal{F}_{\text{D}} = \frac{-\pi^2}{24\sqrt{x}}\left[1 + \left(\frac{1}{24} - \frac{4}{\pi^2}\right)x + \left(\frac{1}{6\pi^2} - \frac{17}{5760}\right)x^2 + \cdots\right], \tag{10}$$

with $x = d/R$, where we have dropped a distance independent constant. At large distance one has

$$\mathcal{F}_{\text{D}} = \frac{1}{2}\ln\left(2\ln\frac{D}{R}\right) - \frac{1}{2(D/R)^2\ln D/R} + \ldots, \tag{11}$$

which is in agreement with Ref. [39].

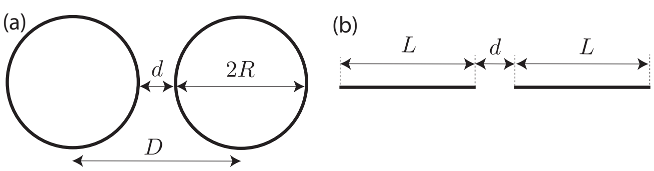

FIG. 2: Relevant length scales for (a) two circles, and (b) two aligned needles.

Next consider two aligned needles of length L and tip-to-tip distance d, as in Fig. 2(b). The conformal map $w(z)$ can be constructed by the Schwarz-Christoffel transformation for polygons [38], and the mutual capacitance is $C = K(\sqrt{1-k^2})/K(k)$ where $K(k)$ is the complete elliptic integral of the first kind, with $k = d/(2L+d)$. Contrary to smooth surfaces, F_{geo} does not go to a constant at short distances for needles which have singular curvature. In this limit, both $\mathcal{F}_{\text{ann.}}$ and $\mathcal{F}_{\text{geo.}}$ scale logarithmically with separation for D and N conditions. At large separation, the geometric component contributes to leading order only for N conditions. The total Casimir force for Dirichlet conditions is given by

$$2L\,F_{\text{D}} = -\frac{1}{2x\ln(8x)} + \frac{1+\ln(8x)}{4x^2\ln^2(8x)} + \mathcal{O}\left(x^{-3}\right), \tag{12}$$

$$2L\,F_{\text{D}} = -\frac{1}{8x} - \frac{1}{8} + \frac{x}{4} + \mathcal{O}\left(x^2\right), \tag{13}$$

for large and small $x = d/(2L)$, respectively. For Neumann conditions the two limits read

$$2L\,F_{\text{N}} = -\frac{1}{512\,x^5} + \frac{5}{1024\,x^6} + \mathcal{O}\left(x^{-7}\right) \tag{14}$$

$$2L\,F_{\text{N}} = -\frac{1}{2x}\left(\frac{1}{4} - \frac{1}{\ln(4/x)}\right) - \frac{1}{8} - \frac{1}{2\ln(4/x)}\left(1 + \frac{1}{\ln(4/x)}\right) + \mathcal{O}(x). \tag{15}$$

Figure 3 depicts the above asymptotic limits as dashed curves, together with the exact result obtained from Eq. (1) with the map $\tilde{w}(z)$ for two needles (solid curves). For D conditions the few terms of Eqs. (12), (13) give an accurate description at almost all separations.

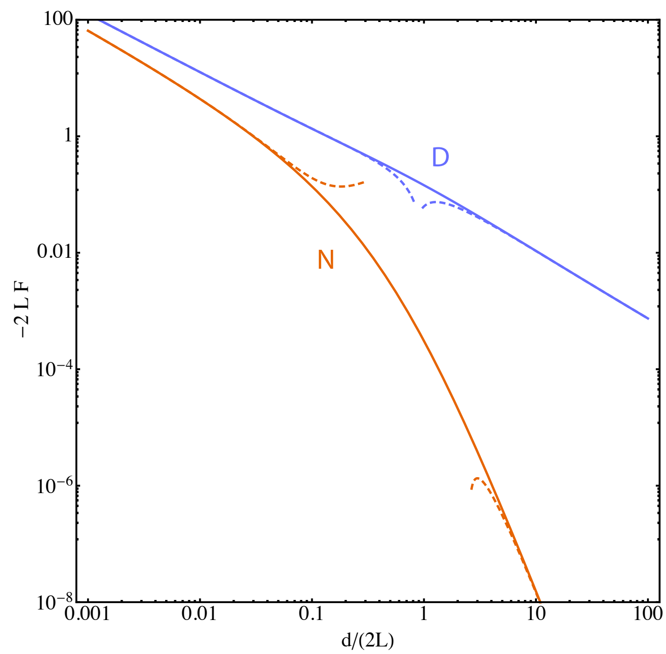

FIG. 3: The Casimir force F between two aligned needles of length L due to a scalar Gaussian field with Dirichlet (D) and Neumann (N) boundary conditions, as a function of the tip-to-tip separation d. Solid curves: exact result; dashed curves: short and large distance expansions from Eqs. (12)–(15).

The above examples nicely demonstrate how the exact form of the Casimir force between two objects of arbitrary shape in a 2D CFT can be obtained in terms of (i) the mutual capacitance C, (ii) the free energy of the CFT on an annulus $\mathcal{F}_{\text{ann.}}$, and (iii) a geometric contribution from the Schwarzian derivative of the map to the annulus $\{\tilde{w}, z\}$. C an be easily computed with high precision numerically; the asymptotic forms of $\mathcal{F}_{\text{ann.}}$ are known for all CFT. The geometric contribution to the force falls off as ζ^{-5} for large separations (for non-circular objects), its short distance behavior is non-trivially dependent on smoothness and other characteristics of the shape. To clarify this intricate shape dependence, calculations for other geometries are on the way. In particular, while not presented here for brevity, we have confirmed the $1/d$ divergence of $F_{\rm geo}$ for finite wedges of arbitrary angle.

We thank R. L. Jaffe and B. Duplantier for valuable discussions. This research was supported by the ESF Research Network CASIMIR, Labex PALM AO 2013 grant CASIMIR, and the NSF through grant No. DMR-12-06323.

[1] M. Kardar and R. Golestanian, Rev. Mod. Phys. **71**, 1233 (1999).

[2] V. A. Parsegian, *Van der Waals Forces* (Cambridge University Press, 2005).

[3] M. Bordag, G. L. Klimchitskaya, U. Mohideen, and V. M. Mostepanenko, *Advances in the Casimir Effect* (Oxford University Press, 2009).

[4] P.-G. de Gennes and M. E. Fisher, C. R. Acad. Sci. Ser. B **287**, 207 (1978).

[5] M. Krech, *The Casimir effect in Critical systems* (World Scientific, 1994).

[6] R. Garcia and M. H. W. Chen, Phys. Rev. Lett. **83**, 1187 (1999).

[7] A. Mukhopadhyay and B. M. Law, Phys. Rev. Lett. **83**, 772 (1999).

[8] M. Fukuto, Y. F. Yano, and P. S. Pershan, Phys. Rev. Lett. **94**, 135702 (2005).

[9] C. Hertlein, L. Helden, A. Gambassi, S. Dietrich, and C. Bechinger, Nature **451**, 172 (2008).

[10] F. Soyka, O. Zvyagolskaya, C. Hertlein, L. Helden, and C. Bechinger, Phys. Rev. Lett. **101**, 208301 (2008).

[11] S. L. Veatch, O. Soubias, S. L. Keller, and K. Gawrisch, Proc. Natl. Acad. Sci. U.S.A. **104**, 17650 (2007).

[12] T. Baumgart, A. T. Hammond, P. Sengupta, S. T. Hess, D. A. Holowka, B. A. Baird, and W. W. Webb, Proc. Natl. Acad. Sci. U.S.A. **104**, 3165 (2007).

[13] B. B. Machta, S. L. Veatch, and J. Sethna, Phys. Rev. Lett. **109**, 138101 (2012).

[14] D. R. Nelson, T. Piran, and S. Weinberg, *Statistical Mechanics of Membranes and Surfaces* (World Scientific, 1989).

[15] M. Goulian, R. Bruinsma, and P. Pincus, Euro. Phys. Lett. **22**, 145 (1993).

[16] R. Golestanian, M. Goulian, and M. Kardar, Phys. Rev. E **54**, 6725 (1996).

[17] F. Bresme and M. Oettel, J. Phys.: Condens. Matter **19**, 413101 (2007).

[18] C. Yolcu, I. Z. Rothstein, and M. Deserno, Phys. Rev. E **85**, 011140 (2012).

[19] E. Noruzifar, J. Wagner, and R. Zandi, Preprint arXiv:1306.4718 (2013).

[20] N. Weil and O. Farago, Phys. Rev. E **84**, 051907 (2011).

[21] D. Friedan, Z. Qui, and S. Shenker, Phys. Rev. Lett. **52**, 1575 (1984).

[22] J. L. Cardy, in *Fields, Strings, and Critical Phenomena*, edited by E. Brézin and J. Zinn-Justin (Elsevier, New York, 1989).

[23] J. Cardy, Nucl. Phys. B **275**, 200 (1986).

[24] P. Kleban and I. Vassileva, J. Phys. A: Math. Gen. **24**, 3407 (1991).

[25] P. Kleban and I. Peschel, Z. Phys. B **101**, 447 (1996).

[26] T. W. Burkhardt and E. Eisenriegler, Phys. Rev. Lett. **74**, 3189 (1995).

[27] E. Eisenriegler and U. Ritschel, Phys. Rev. B **51**, 13717 (1995).

[28] E. Eisenriegler, J. Chem. Phys. **121**, 3299 (2004).

[29] E. Eisenriegler, J. Chem. Phys. **124**, 144912 (2006).

[30] I. Z. Rothstein, Nucl. Phys. B **862**, 576 (2012).

[31] O. A. Vasilyev, E. Eisenriegler, and S. Dietrich, Preprint arXiv:1304.4220 (2012).

[32] G. Bimonte and T. Emig, Phys. Rev. Lett. **109**, 160403 (2012).

[33] R. Courant, *Dirichlet's principle, conformal mapping and minimal surfaces* (Interscience Publishers, 1950).

[34] P. di Francesco, P. Mathieu, and D. Sénéchal, *Conformal Field Theory* (Springer, 1997).

[35] Z. Nehari, *Conformal Mapping* (Dover, 1952).

[36] S. J. Rahi, T. Emig, N. Graham, R. L. Jaffe, and M. Kardar, Phys. Rev. D **80**, 085021 (2009).

[37] B. Derjaguin, Kolloid Z. **69**, 155 (1934).

[38] W. R. Smythe, *Static and dynamic electricity* (McGraw-Hill, 1950).

[39] H. Lehle, M. Oettel, and S. Dietrich, Europhys. Lett. **75**, 174 (2006).

[40] A Jordan curve is any non-intersecting closed planar trajectory.

[41] Here it is assumed that the spectrum of $\hat{L}_0+\hat{\bar{L}}_0$ is discrete which is not necessarily the case for $c \geq 1$.